https://doi.org/10.5194/wes-2026-70
Preprint. Discussion started: 23 April 2026

eawe european academy of wind energy
Open Access WIND ENERGY SCIENCE DISCUSSIONS

Machine Learning Framework for Scour Detection Across Multiple Offshore Wind Farms

Mahmoud Abdelhak[1*], Luke J Prendergast [2], Jacques Tott-Buswell [2], Ramin Ghiasi [1], Abdollah Malekjafarian [1]

[1]Structural Dynamics and Assessment Laboratory, School of Civil Engineering, University College Dublin, Dublin, Ireland.
[2]University of Nottingham, Department of Civil Engineering, Nottingham, NG7 2RD, United Kingdom
Correspondence to: mahmoud.abdelhak@ucdconnect.ie)

Abstract.

This paper proposes a global scour detection framework for monopile foundations across offshore wind farms, based on data from a single accelerometer installed on the turbine tower. The framework is designed to address the real-world complexity and heterogeneity of offshore wind systems installed across multiple offshore sites. To achieve this, numerically generated acceleration data are obtained for various offshore wind turbines (OWTs) across multiple wind farms using a coupled OpenFAST and bespoke soil-structure interaction (SSI) model. The simulation accounts for a wide array of offshore conditions, from sea states and soil properties to structural characteristics and site-specific scour. For each OWT, acceleration data are generated using foundation stiffness derived from the SSI model, reflecting the site conditions and turbine characteristics. A multi-source domain generalisation (DG) strategy is then employed, in which a model trained on a combined dataset containing one turbine per farm (referred to as source turbines) is used to detect scour around the remaining, previously unseen turbines (referred to as target turbines) across geographically-disparate wind farms. The results demonstrate that the proposed method can identify the scour state for multiple target turbines across multiple wind farms with acceptable accuracy. In addition, the choice of source turbine significantly impacts model performance, with shallow water, low-stiffness turbine foundations providing the most reliable training base. Furthermore, obtaining sensor data from the tower base significantly improves scour detection, while increasing the number of source turbines in the training dataset enhances prediction accuracy, specifically at lower scour states.

Keywords: Machine Learning, Vibrational analysis, Scour detection, Structural Health Monitoring, Domain Generalisation, Monopile.

1 Introduction

Monopile foundations support the majority of installed offshore wind turbines (OWT); however, they are vulnerable to several issues, including corrosion, fatigue, boat collisions, and scour (Wang et al., 2018). Scour, in particular, occurs due to soil erosion around the foundation caused by wave and current interactions (Duan et al., 2025). It can result in severe impacts on the structural and dynamic behaviour of monopile foundations, leading to excessive lateral pile head displacement (Mostafa, 2012) and increased bending moments (Lin et al., 2016). Additionally, scour causes a notable reduction in the natural frequency

https://doi.org/10.5194/wes-2026-70
Preprint. Discussion started: 23 April 2026

eawe european academy of wind energy
Open Access WIND ENERGY SCIENCE DISCUSSIONS

(Niu et al., 2023; Prendergast et al., 2015) and changes in the tower's mode shapes (Niu et al., 2023). Many studies have investigated scour detection using a vibrational-based method (Dai et al., 2021; Niu et al., 2023; Prendergast et al., 2018; Weijtjens et al., 2017). These works primarily examined dynamic response characteristics, such as natural frequencies, mode shapes, and damping ratios, and investigated their usage as indicators for scour occurrence. A common finding is that the low probability of detecting shallow scour depths using frequency measurements arises from the difficulty in distinguishing minor frequency shifts caused by shallow scour from those induced by environmental conditions (Abdelhak et al., 2025).

Recent developments in Structural Health Monitoring (SHM) and Machine Learning (ML), specifically data-driven approaches, have demonstrated a strong potential for enhancing scour detection methods. In this context, several studies have applied data-driven approaches for scour detection, yielding promising results. For example, Jawalageri et al., (2024) proposed a data-driven approach using a Naïve Bayes model, trained on labelled acceleration data, to classify scour depths around monopile foundations supporting an NREL 5 MW OWT. Extending beyond acceleration data, Jeong et al., (2020) proposed a data fusion approach, which combined both acceleration and angular velocity responses to predict scour occurrence. Similarly, Jatoliya et al., (2024) applied various ML models to predict scour hole depths, while Lu et al., (2024) integrated scour physics and video processing techniques to improve scour detection capabilities. In addition, Najafzadeh et al., (2025) proposed ML approaches to estimate the severity of scour damage in protected monopile foundations. By evaluating five ML algorithms - Random Forest (RF), Support Vector Machine (SVM), Extreme Gradient Boosting (XGBoost), Adaptive Boosting (AdaBoost), and Categorical Boosting (CatBoost) - they demonstrated that ML techniques can effectively assess damage severity in scour protection systems. Despite their success in detecting scour around single turbines, these approaches primarily rely on supervised learning models, which require access to labelled data −a process that is expensive and time-consuming. Abdelhak et al., (2025) addressed this limitation by developing an unsupervised approach which trained a One-Class SVM on healthy acceleration data to detect scour around OWTs with unlabelled data. Their results demonstrated strong potential for identifying scour around monopile foundations under varying environmental conditions without access to scour damage labels. Models trained with larger and more diverse datasets with environmental variability outperformed those developed under limited conditions. Despite these advances, previous studies have mainly focused on scour detection for individual turbines under site-specific conditions, requiring a separate model for each turbine. Additionally, these approaches rely on multiple data sensors distributed along the tower, which increases installation costs and requires comprehensive monitoring systems.

Traditional Machine Learning (TML) techniques used for scour detection are usually evaluated on datasets collected from the same turbine used for model development. However, applying these models to datasets from other turbines results in a significant performance drop, driven by shifts in the underlying data distribution (Teng et al., 2022). This limitation restricts practical applicability, as offshore wind farms comprise multiple turbines with diverse site-specific conditions and scour levels. These variations introduce significant distributional shifts between turbine datasets, increasing the complexity of large-scale scour detection. A scour detection-based Domain Adaptation (DA) approach, proposed by Abdelhak et al., (2025), shows a strong potential for scour detection at the farm level. Primarily, DA addresses domain shift by aligning the distributions of the source and target turbine data. Despite being trained exclusively on numerically-generated healthy data from a single turbine, the Geodesic Flow Kernel (GFK) technique demonstrates high accuracy in predicting the foundation status (healthy or scoured) of multiple turbines across a hypothetical offshore wind farm. However, this technique requires target turbine data during the training phase, necessitating the installation of a data acquisition system on both source and target turbines. While practical for a single wind farm when the target data are included in training, its applicability across multiple farms is limited when such data are unavailable. Consequently, data access during model development remains a critical challenge for the practical application of DA-based scour detection methods at the inter-farm level. To generalise scour detection across wind farms with limited data availability, domain generalisation (DG) techniques can be employed to transfer knowledge from multi-source

https://doi.org/10.5194/wes-2026-70
Preprint. Discussion started: 23 April 2026

eawe european academy of wind energy
Open Access WIND ENERGY SCIENCE DISCUSSIONS

turbines to previously unseen target turbines. This is achieved by learning domain-invariant features from the source turbines, enabling accurate prediction at unseen target turbines.

To enhance the generalisability of scour detection across multiple wind farms, this study proposes a global scour detection framework based on multi-source DG techniques, trained on a combined dataset containing one source turbine per farm and designed to detect scour in the remaining, previously unseen target turbines across these farms. The proposed approach relies on single sensor measurements, specifically Power Spectral Density (PSD) features derived from acceleration data collected at the OWT tower. The DG framework is implemented using a Domain-Adversarial Neural Network (DANN) technique, trained on data from a single reference turbine per farm, assumed to represent the early life stage and including labelled healthy and shallow scour states (1m depth). Despite relying on lightly instrumented source turbines, the framework demonstrates the capability to detect multiple scour levels across geographically varying offshore wind farms. Moreover, the study investigates the sensitivity of model performance to the volume of source data (the number of source turbines). The effectiveness of alternative DG methods, such as Causal Disentanglement Domain Generalisation (CDDG), is furthermore evaluated to further validate the proposed methodology.

2. Methodology

This study proposes a generalised scour detection framework at the inter-wind farm scale. In this framework, a model trained on labelled data from individual source turbines −each located at a specific farm (e.g. Farm 1, Farm 2, and Farm 3) −is used to identify the scour condition of previously unseen target turbines installed across these farms. An overview of the proposed methodology is briefly described in Figure 1, where source turbines are indicated by red boxes and target turbines by green boxes. The source turbines are assumed to provide early life acceleration data containing healthy and shallow scour states. For each source turbine, acceleration data are numerically generated using an integrated OpenFAST and soil structure interaction (SSI) model developed in MATLAB. The data are obtained from a single accelerometer (represented as a node point in the numerical model) located on the OWT tower. The resulting datasets are processed to extract PSD features, which are then normalised and batched to facilitate latent feature extraction and serve as the foundation for training a domain generalisation-based scour detection model. More details about DG methods can be found in Section 2.1, with the DANN method selected for model development. The architecture and training of DANN are described in Section 2.2. The trained model is first validated on source turbines to ensure satisfactory performance before being applied to predict scour conditions at target turbines. Various training protocols, outlined in Section 2.4, are incorporated to enhance the model's generalisation capability across multiple wind farms. The proposed methodology aims to reduce the number of sensors required for condition monitoring at the inter-wind farm level.

https://doi.org/10.5194/wes-2026-70
Preprint. Discussion started: 23 April 2026

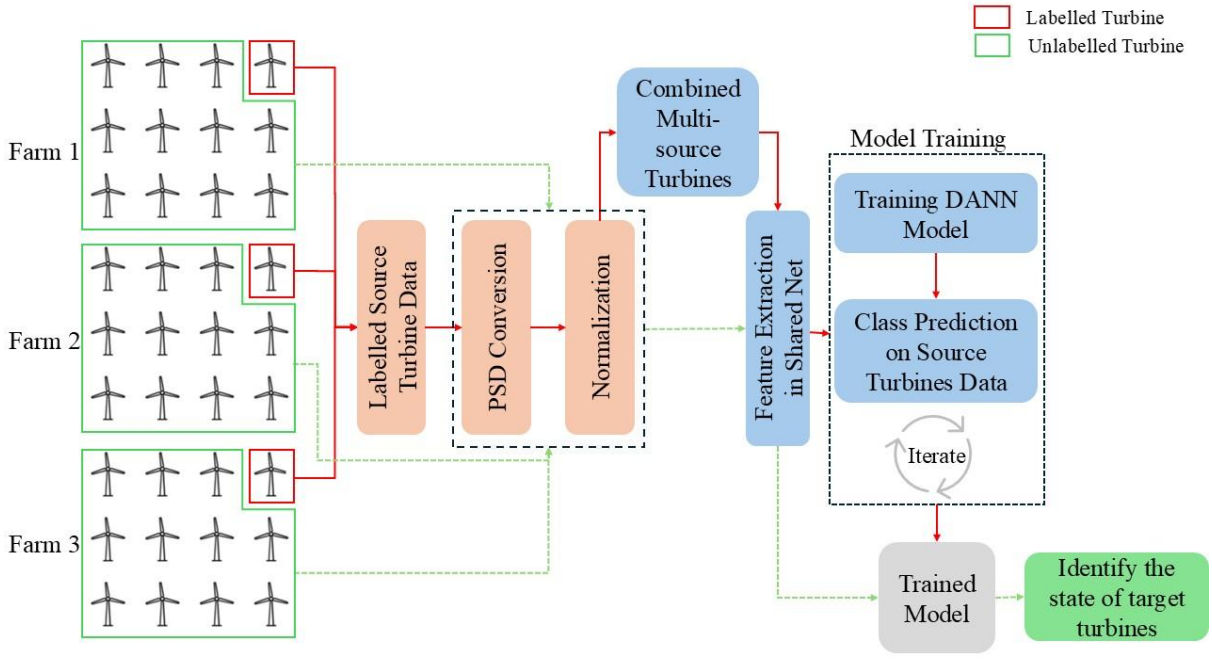

Figure 1: Conceptual schematic of the proposed multi-farm scour detection framework

2.1 Domain generalisation

DG can be implemented through several approaches, including adversarial training, metric learning, meta-learning and integrated learning techniques, all aimed at extracting domain invariant features across different operating conditions (Dayal et al., 2023). In the context of fault diagnosis in engineering systems, DG provided a strong potential for robust damage detection (Cao et al., 2025). Accordingly, several studies applied DG models to transfer the fault knowledge from multiple source domains to unseen target domains. For instance, Li et al., (2020) proposed a domain generalisation method based on adversarial training for fault diagnosis in rotating machinery, while Jia et al., (2023) developed a causality-based approach that decomposes fault features to achieve more reliable domain-generalised diagnosis.

For a detailed description of DG model based scour detection at farm -level, the source turbines can be represented as $D_s = \{D_s^1, D_s^2, \dots, D_s^c\}$, where c is the number of the source turbines (or domains). Each source turbine dataset is defined as $D_s^c = \{(x_i^c, y_i^c)\}_{i=1}^{N_c}$, where N_c is the number of the labelled samples, $x_i^c \in X$ denotes the feature vector, and $y_i^c \in Y$ demonstrates the corresponding class label. Similarly, a target turbine dataset can be defined as $D_t = \{(x_j^t)\}_{j=1}^{N_t}$ where N_t is the number of samples in the target domain x_j^t denotes the number of samples in the target turbine. In this study, the source turbine has a labelled dataset, whereas the target labels y_j^t are assumed to be unavailable during training. Importantly, each farm has an individual reference turbine from a different wind farm, characterised by unique site-specific conditions. Consequently, both marginal and conditional distributions vary across domains such that $P(X_s^1) \neq P(X_s^2) \neq P(X_t)$, and $P(Y_s^1 \mid X_s^1) \neq P(Y_s^2 \mid X_s^2) \neq \cdots P(Y_t \mid X_t)$, where $P(X_s)$ denotes the marginal distribution of the source features and $P(Y_s \mid X_s)$ represents their conditional distribution. For each source turbine, the feature space X_s, and label space Y_s are defined, forming the joint distribution $P(X_s, Y_s)$. Thus, the generalised joint distribution can be defined as $P^m(X_s, Y_s)$ where $P_{X_s}^m$ denotes the marginal distribution with m representing the number of source turbines. In this study, the labelled source turbine has two class labels

https://doi.org/10.5194/wes-2026-70
Preprint. Discussion started: 23 April 2026

(healthy and scoured), with the source dataset contains N_s =1440 samples, divided equally between the two classes. Given datasets from N_s source turbines, the objective of domain generalisation is to learn a predictive function that minimises the generalisation error on unseen target turbines.

2.2 Domain-Adversarial Neural Network (DANN)

DANN mainly incorporates an adversarial training strategy based on a domain discriminator to encourage indistinguishability between features extracted from different domains (Ju et al., 2025). Although DANN is commonly used for domain adaptation, this study adapted it for domain generalisation by training the model to extract domain-invariant features. In this framework, the adversarial training process simultaneously optimises two objectives: a feature extractor, which trains to generate domain-invariant features that enable accurate classification of scour states, and a domain discriminator, which attempts to identify the source domain for each sample. Figure 2 demonstrates the architecture of the DANN technique, consisting of three main components as described by Ganin et al., (2014): a feature extractor network, a task-specific classifier, and a domain discriminator. It employs a multi-class domain discriminator that learns to distinguish between source domains based on the feature representations. Meanwhile, the feature extractor is optimised to both support the task-specific classifier and simultaneously confuse the domain discriminator, thereby encouraging the model to learn domain-invariant features. This adversarial interaction is employed through the Gradient Reversal Layer (GRL), which reverses the gradient during backpropagation to the feature extractor. Therefore, the discriminator becomes less effective at determining the source domain of a given sample, while the extractor learns invariant features across domains, which are valuable for scour classification.

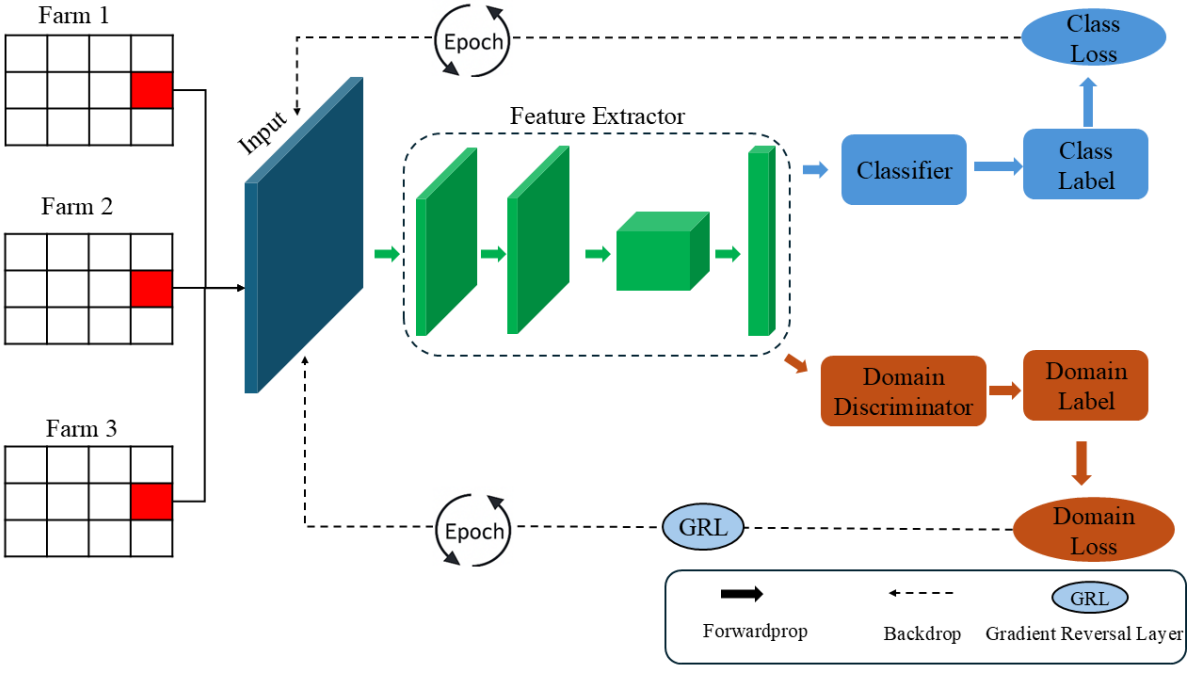

Figure 2: Architecture of the DANN method for DG

The DANN model is designed to learn class-discriminative features and domain-invariant representations through joint adversarial training. Table 1 illustrates the architecture of the feature extractor, designed as a 1D Convolutional Neural Network (CNN), and its corresponding classifier. It consists of four convolutional layers, each followed by a max-pooling layer, and

https://doi.org/10.5194/wes-2026-70
Preprint. Discussion started: 23 April 2026

uses PSD features as input. Following the final convolutional block, the feature signals are flattened, resulting in a 256-dimensional latent feature vector per sample. The fully connected layer then maps these latent features to the output classes (healthy vs. scoured), which are optimised using a cross-entropy classification loss to ensure strong discriminative ability in the source turbines. In contrast, the adversarial domain classifier uses latent features to predict the turbine labels (source turbine 1, 2, or 3). The adversarial domain classifier is further trained using an adversarial loss function, implemented via a GRL layer, to encourage the shared network to produce domain-invariant features, thereby enhancing generalisation across unseen domains.

Table 1: Architecture of feature extractor and classifier

Module	Layer type	Kernel number	Kernel size	Stride	Activation	Normalization
Feature Extractor (CNN)	Convolution	16	64 x 1	1	ReLU	Batch Normalization
	Max-pooling	–	2 x 1	2	–	–
	Convolution	32	16 x 1	1	ReLU	Batch Normalization
	Max-pooling	–	2 x 1	2	–	–
	Convolution	64	5 x 1	1	ReLU	Batch Normalization
	Max-pooling	–	2 x 1	2	–	–
	Convolution	64	5 x 1	1	ReLU	Batch Normalization
	Max-pooling	–	2 x 1	2	–	–
Classifier	Fully Connected	–	Class number (2)	–	Softmax	–

2.3 Training and evaluation protocols

Scour primarily affects the dynamic behaviour of OWTs by changing the foundation stiffness as soil around the monopile is removed. In the time domain representations, the acceleration signals show a negligible impact of scour due to their low-frequency bandwidth. However, the changes in the dynamic performance of OWTs due to scour become more obvious in the frequency domain, making frequency-domain features more suitable for scour detection [31]. Accordingly, the logarithmic PSD of the acceleration data is used to train the DANN model for generalising scour detection across offshore wind farms. Notably, the PSD range is limited to frequency regions with high energy content (0-8 Hz), excluding those with minimal contribution. In this study, multiple training protocols are designed to evaluate the robustness of the proposed approach under multiple scenarios of data availability. Several training protocols are investigated, including training on consistent source turbines, located at sites with minimum, intermediate, and maximum water depths, and soil densities within the wind farm. In Protocol 1, the model is trained using data from source turbines located in shallow water with low soil density (Turbine 1 across different farms). Protocol 2 uses source turbines located at an intermediate water level and medium soil density (Turbine 6 across different farms). In Protocol 3, the source turbines are located at the deepest water conditions and highest soil density. In addition to these scenarios with consistent water depth across source turbines, an additional protocol is introduced to examine cases where the source turbines operate at varying water depths. Moreover, an extended training protocol is introduced to reduce domain mismatch through incorporating data from six turbines spanning shallow and intermediate water depths. This

https://doi.org/10.5194/wes-2026-70
Preprint. Discussion started: 23 April 2026

eawe european academy of wind energy
Open Access WIND ENERGY SCIENCE DISCUSSIONS

protocol also integrates a target normalisation scheme, where target turbine datasets are normalised relative to the closest reference source turbine.

Across different training protocols, a consistent evaluation is applied, where the trained model is systematically evaluated on the remaining previously unseen target turbines within the wind farms, regardless of their location or relative distance from the source turbines. Importantly, each target turbine has unique site specifications and is subjected to different levels of scour, ranging from shallow scour depths (S =1 – 3 m, ≈ $0.5D$), intermediate scour depths (S = 4 – 6 m, ≈ $1.0D$), and deep scour depths (S = 7 – 9 m, ≈ $1.5D$), where S represents scour depth while D denotes the monopile diameter. Notably, the scour in this study is mainly characterised by scour depth because of its significant impact on the dynamic characteristics of the system, while other scour hole parameters, such as width and slope, are neglected due to their minor impacts. A simple accuracy metric, defined as the ratio of correctly predicted samples to the total number of target samples, is used for model evaluation. For example, a 50% accuracy indicates that the model fails to distinguish between classes and is biased to a single state (either all healthy or all scoured), whereas 100% reflects the correct prediction of all samples.

3. Data generation

This study adopts the NREL 5 MW offshore wind turbine (Jonkman et al., 2009) as the reference model for data generation. A comprehensive overview of the structural parameters is provided in Table 2.

Table 2: NREL 5 MW OWT properties (Jonkman et al., 2009)

Description	Value
Rating	5 MW
Configuration	3 blades
Rotor, hub diameter	126 m, 3 m
Hub height	90 m
Rated rotor speed	12.1 rpm
Rotor mass	110,000 kg
Nacelle mass	240,000 kg
Tower mass	347,500 kg
MP Diameter	6.0 m
MP wall thicknesses	0.060 m (above mudline)
Tower top diameter, wall thickness	3.87 m, 0.019 m
Tower base diameter, wall thickness	6.0 m, 0.027 m
Support structure steel density	8500 kg/m^3
Steel Young's modulus	210 GPa
Steel Shear modulus	80.8 GPa

https://doi.org/10.5194/wes-2026-70
Preprint. Discussion started: 23 April 2026

eawe european academy of wind energy
Open Access WIND ENERGY SCIENCE DISCUSSIONS

3.1 Foundation specifications across wind farms

This study is performed using numerically generated data assumed to be obtained from three medium-sized farms, each consisting of 11 turbine units. The farms are assumed to be located in areas with different soil types, including dense sand, medium-dense sand, and loose sand. The offshore wind farms are referred to as Farm 1, Farm 2, and Farm 3 in subsequent analyses, where each farm has monopile foundations which designed according to their site-specific soil characteristics. Across a single farm, multiple turbines are installed in water depths ranging from 20 m to 25 m, with changes in soil conditions to capture the influences of local soil heterogeneity on structural response. In addition, the monopile dimensions are adjusted at each location to fulfil the required safety and design criteria (Arany et al., 2017). Table 3 indicates the foundation specifications of OWTs at Farm 1. For example, Farm 1 comprises monopiles with a consistent diameter of 6 m and a length of 30 m, with slightly varying wall thickness to achieve the design requirements.

Table 3: Key Specifications of OWT Foundations at Farm 1

Unit Name	Water Depth (m)	Soil Relative Density	Soil Unit Weight (kN/m^3)	Pile Diameter (m)	Wall Thickness (mm)	Embedment Depth (m)
T1.1	20.0	0.70	19.0	6	85	30
T1.2	20.5	0.72	19.1	6	85	30
T1.3	21.0	0.74	19.2	6	85	30
T1.4	21.5	0.76	19.3	6	90	30
T1.5	220	0.78	19.4	6	90	30
T1.6	22.5	0.80	19.5	6	90	30
T1.7	23.0	0.82	19.6	6	90	30
T1.8	23.5	0.84	19.7	6	95	30
T1.9	24.0	0.86	19.8	6	95	30
T1.10	24.5	0.88	19.9	6	95	30
T1.11	25.0	0.90	20.0	6	95	30

Table 4 presents the key specifications for monopile foundations at Farm 2, which is assumed to be located in medium-dense sand. Unlike Farm 1, the pile diameter at this farm varies slightly between turbines, ranging from 6.0 m to 6.2 m, while the wall thickness is kept constant at 90 mm to meet the design criteria. Whereas an embedment depth of 40 m is adopted according to Ref (Arany et al., 2017).

Table 4:Key Specifications of OWT Foundations at Farm 2

Unit Name	Water Depth (m)	Soil Relative Density	Soil Unit Weight (kN/m^3)	Pile Diameter (m)	Wall Thickness (mm)	Embedment Depth (m)
T2.1	20.0	0.40	18.0	6.0	90	40
T2.2	20.5	0.42	18.1	6.0	90	40
T2.3	21.0	0.44	18.2	6.0	90	40

https://doi.org/10.5194/wes-2026-70
Preprint. Discussion started: 23 April 2026

eawe european academy of wind energy
Open Access WIND ENERGY SCIENCE DISCUSSIONS

T2.4	21.5	0.46	18.3	6.0	90	40
T2.5	220	0.48	18.4	6.0	90	40
T2.6	22.5	0.50	18.5	6.1	90	40
T2.7	23.0	0.52	18.6	6.1	90	40
T2.8	23.5	0.54	18.7	6.1	90	40
T2.9	24.0	0.56	18.8	6.1	90	40
T2.10	24.5	0.58	18.9	6.2	90	40
T2.11	25.0	0.60	19.0	6.2	90	40

Table 5 reports the monopile foundation specifications for Farm 3. This farm has a varying pile diameter while maintaining a constant wall thickness, and an embedment depth of 50 m is used across all turbines.

Table 5: Key Specifications of OWT Foundations at Farm 3

Unit Name	Water Depth (m)	Soil Relative Density	Soil Unit Weight (kN/m^3)	Pile Diameter (m)	Wall Thickness (mm)	Embedment Depth (m)
T3.1	20.0	0.20	17.0	6.0	90	50
T3.2	20.5	0.22	17.1	6.0	90	50
T3.3	21.0	0.24	17.2	6.0	90	50
T3.4	21.5	0.26	17.3	6.0	90	50
T3.5	22.0	0.28	17.4	6.0	90	50
T3.6	22.5	0.30	17.5	6.1	90	50
T3.7	23.0	0.32	17.6	6.1	90	50
T3.8	23.5	0.34	17.7	6.1	90	50
T3.9	24.0	0.36	17.8	6.1	90	50
T3.10	24.5	0.38	17.9	6.2	90	50
T3.11	25.0	0.40	18.0	6.2	90	50

3.2 Environmental conditions

Due to the variation in installation locations, each wind farm is assumed to experience distinct environmental conditions, which aligns with the realistic representation of real-world situations. Each farm operates under 12 Load Cases (LCs) encompassing variations in wind speed, wave height, and wave period. All farms are assumed to be located at the Celtic Sea, where only a single buoy (M5, near Wicklow) provides measured data (Huang et al., 2021). To account for farm-specific environmental variability, historical buoy measurements over different years are assigned to each farm, ensuring farm-based conditions. Farm 1 is simulated based on 2022 records, Farm 2 is simulated under 2023 records, while Farm 3 is simulated under 2024 records. To capture the highest occurrence scenarios, the environmental conditions are restricted to the 5th- 95th percentile range, excluding extreme outliers. A linear regression is performed to correlate the wind speed and wave height. The wind speed range captures different operational conditions of the turbine, and the corresponding sea state records provide the associated

https://doi.org/10.5194/wes-2026-70
Preprint. Discussion started: 23 April 2026

eawe european academy of wind energy
Open Access WIND ENERGY SCIENCE DISCUSSIONS

225 wave height and period. However, the available dataset is limited with respect to sea current measurements. Therefore, the DNV-GL current model (DNV-GL, 2016) is used to estimate the sea surface current speed as a function of the wind speed at the 10 m level above the sea level. It is important to note that the water depth at the buoy location may differ from that assumed for the wind farms due to the limited availability of environmental data at the required depth. Table 6-8 show the environmental conditions for Farms 1-3, respectively.

230 **Table 6: Environmental Conditions at Farm 1**

Load Case	Wind Speed (m/s)	Wave Height (m)	Wave Period (second)	Current Speed (m/s)
LC 1.1	10.0	1.61	5.14	0.26
LC 1.2	11.0	1.73	5.23	0.29
LC 1.3	11.5	1.79	5.28	0.30
LC 1.4	12.0	1.85	5.32	0.31
LC 1.5	12.5	1.91	5.37	0.32
LC 1.6	13.0	1.97	5.41	0.34
LC 1.7	13.5	2.03	5.46	0.35
LC 1.8	14.0	2.09	5.50	0.36
LC 1.9	14.5	2.15	5.55	0.38
LC 1.10	15.0	2.21	5.59	0.39
LC 1.11	15.5	2.27	5.64	0.40
LC 1.12	16.0	2.33	5.68	0.41

Table 7: Environmental Conditions at Farm 2

Load Case	Wind Speed (m/s)	Wave Height (m)	Wave Period (second)	Current Speed (m/s)
LC 2.1	9.60	1.64	5.16	0.25
LC 2.2	10.2	1.73	5.23	0.26
LC 2.3	10.8	1.81	5.30	0.28
LC 2.4	11.4	1.90	5.37	0.30
LC 2.5	12.0	1.98	5.44	0.31
LC 2.6	12.6	2.07	5.51	0.33
LC 2.7	13.2	2.15	5.58	0.34
LC 2.8	13.8	2.24	5.65	0.36
LC 2.9	14.4	2.32	5.72	0.37
LC 2.10	15.0	2.41	5.79	0.39
LC 2.11	15.6	2.49	5.86	0.40
LC 2.12	16.2	2.58	5.94	0.42

Table 8: Environmental Conditions at Farm 3

Load Case	Wind Speed (m/s)	Wave Height (m)	Wave Period (second)	Current Speed (m/s)
LC 3.1	9.30	1.60	5.13	0.24
LC3.2	9.90	1.69	5.20	0.26
LC 3.3	10.5	1.77	5.27	0.27
LC 3.4	11.1	1.86	5.34	0.29

https://doi.org/10.5194/wes-2026-70
Preprint. Discussion started: 23 April 2026

eawe european academy of wind energy
Open Access WIND ENERGY SCIENCE DISCUSSIONS

LC 3.5	11.7	1.94	5.41	0.30
LC 3.6	12.3	2.03	5.48	0.32
LC 3.7	12.9	2.11	5.55	0.33
LC 3.8	13.5	2.19	5.62	0.35
LC 3.9	14.1	2.28	5.69	0.37
LC 3.10	14.7	2.36	5.76	0.38
LC 3.11	15.3	2.45	5.83	0.40
LC 3.12	15.9	2.53	5.90	0.41

To validate the proposed approach, numerical acceleration data were generated using an integrated OpenFAST and SSI model, developed in MATLAB. For more details on the data generation process, refer to Ref. (Abdelhak et al., 2025). The acceleration data are generated at two sensor locations: sensor 1, located at the tower base, 10 m above sea level, and sensor 2, situated at the tower top, as shown in Figure 3. Both sensor locations are used to extract acceleration signals from OpenFAST under various scenarios across the turbines within the considered farms. For each turbine, a coupled OpenFAST and SSI model is developed to generate acceleration data based on the turbine's structural and site characteristics. Each turbine dataset contains healthy and nine scour states, corresponding to scour depths ($S = 1,\ 2,,\ 9m$), resulting in an extensive farm-scale dataset under varying operational conditions and turbine characteristics. This provides realistic scenarios for model training and evaluation, reflecting the variation of the individual turbines and installation sites.

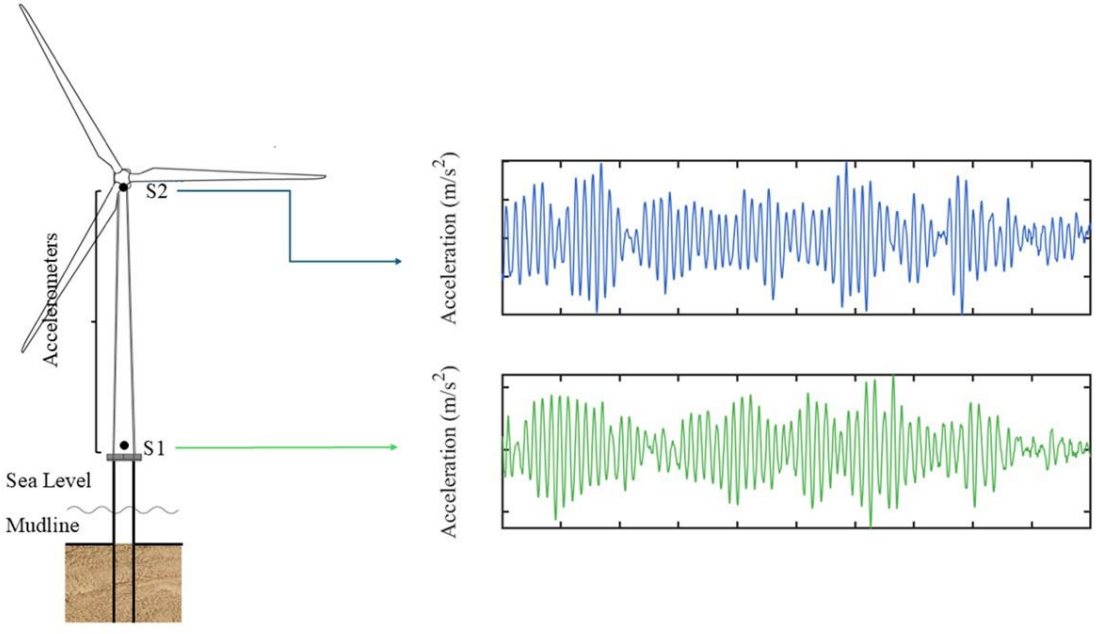

Figure 3: Location of sensors along the tower

3.3 Data preprocessing and loading

The acceleration data generated from the integrated OpenFAST and SSI model have 3600 s per sensor and are sampled at 100 Hz, resulting in 360,000 time instants. Further division of acceleration into fixed-width windows of 6000 time instants was conducted, resulting in 60 windows per LC. Since each turbine is evaluated under 10 scour states, this results in a total of 720 data windows per turbine, obtained from 12 LCs. The PSD of acceleration signals at each window is estimated using Welch's

https://doi.org/10.5194/wes-2026-70
Preprint. Discussion started: 23 April 2026

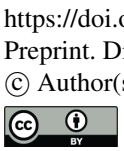

eawe european academy of wind energy
Open Access WIND ENERGY SCIENCE DISCUSSIONS

method (Jwo et al., 2021), with a Hamming window of 1000 points and 50% overlap. The resulting PSDs are trimmed to the first 80 frequency bins to capture the low-frequency range where scour has the most pronounced effect. The extracted PSD features are then converted to a logarithmic scale, after which the source-turbine data are normalised using the minimum and maximum values of the healthy state. These pre-processed features are employed to train the DG model. Figure 4 presents the t-distributed Stochastic Neighbour Embedding (t-SNE) visualisation (Cieslak et al., 2020) of the healthy and scoured state datasets for turbines T1.6, T2.6, and T3.6 in reduced dimension. t-SNE is a nonlinear dimensionality reduction technique that projects high-dimensional data into a low-dimensional space while preserving local similarities between samples. The results indicate the challenge of distinguishing between healthy and scoured states based on the available data, highlighting the complexity of the system and the difficulty of scour detection at the inter-farm scale.

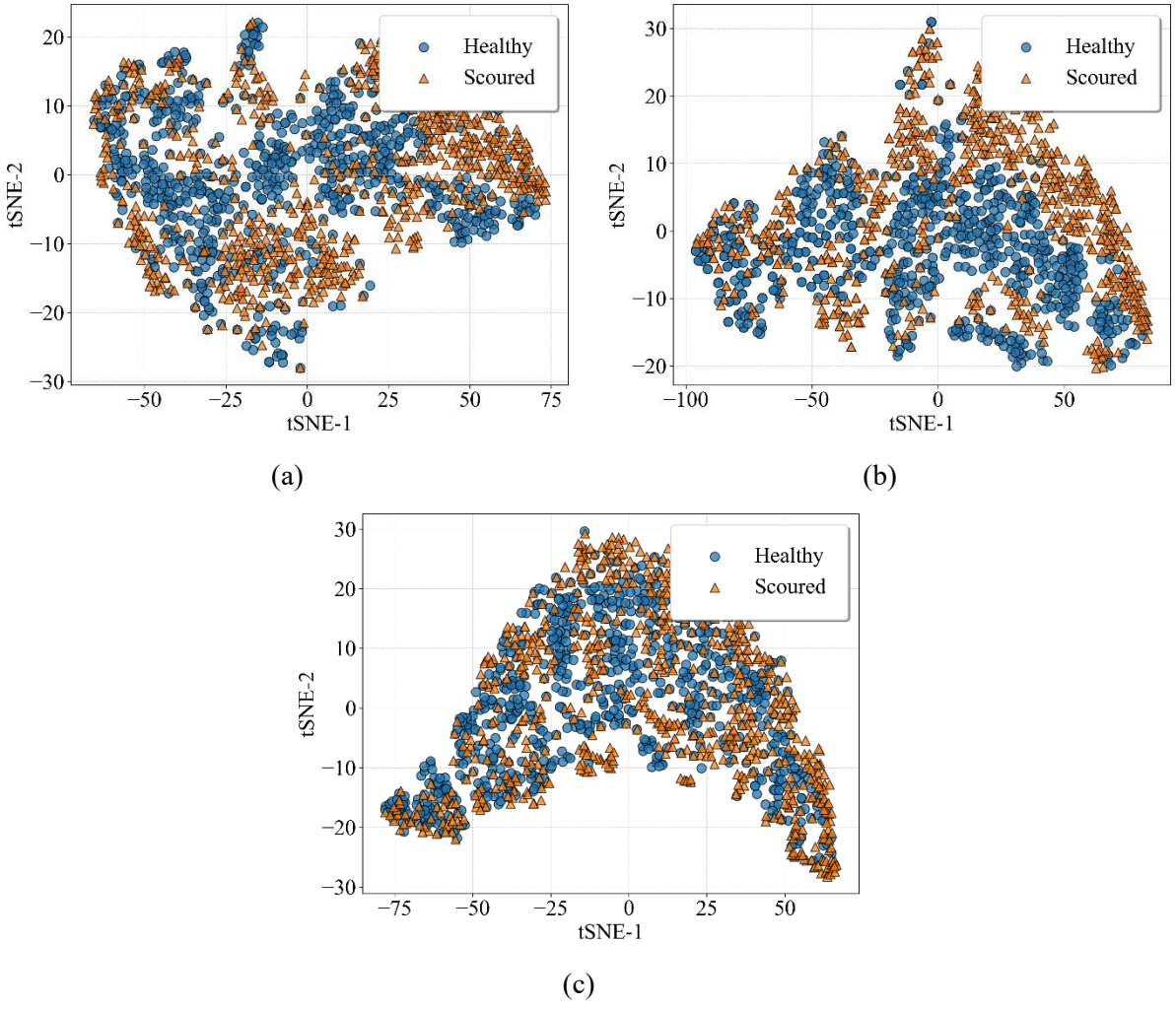

Figure 4: t-SNE distribution for PSD features for turbines a) T1.6, b) T2.6, and c) T3.6 under 2 m scour depth state.

In this study, each sample is assigned dual labels - structural condition (healthy or scoured) and source turbine - enabling the model to simultaneously learn damage-specific features and domain-invariant representations. A training data loader is created

https://doi.org/10.5194/wes-2026-70
Preprint. Discussion started: 23 April 2026

eawe european academy of wind energy
Open Access WIND ENERGY SCIENCE DISCUSSIONS

by combining the feature sets from the three source turbines, with each turbine assigned a distinct domain label (0, 1, or 2) according to its index in the source domains. The feature sets from the three turbines are combined, and their corresponding conditions and domain labels are concatenated into a single, unified label set for model training.

3.4 Similarity study between OWT units across farms

A similarity study was conducted between the source and target turbines within each farm using the Maximum Mean Discrepancy (MMD) metric (Ghojogh et al., 2024). MMD is a statistical metric primarily used to estimate the difference between two probability distributions −in this case, the PSD feature distributions of the source and target turbines. It evaluates the domain similarity by comparing their mean embeddings in a reproducing kernel Hilbert space (RKHS) (Ghojogh et al., 2021). Table 9 reports the MMD distances between the healthy-state data of turbine T1.1 in Farm 1 and the data of the remaining turbines under different scour conditions. Table 10 provides the corresponding results for turbine T2.1 in Farm 2, while Table 11 provides the equivalent results for turbine T3.1 in Farm 3. The results reflect a significant difference between source and target turbine data within each farm, primarily due to variations in soil types, water depth, and structural configuration, all of which alter the system's dynamic performance. These factors contribute to considerable overlap between the healthy and scoured states across turbines within a farm. The intersection in turbines' data distribution across different states demonstrates the complexity of farm-scale scour detection, where each turbine is site-based and affected by changes in the offshore environment.

Table 9: MMD value between the healthy state data of turbine T1.1 and the remaining turbines at Farm 1 under both healthy and scoured states

Scour Depth	Target Turbines										
	T 1.1	T 1.2	T 1.3	T 1.4	T 1.5	T 1.6	T 1.7	T 1.8	T 1.9	T 1.10	T 1.11
0m (Healthy)	0.00	0.02	0.12	0.20	0.32	0.28	0.36	0.44	0.48	0.52	0.52
1m	0.05	0.02	0.03	0.07	0.22	0.18	0.30	0.39	0.42	0.45	0.45
2m	0.25	0.16	0.06	0.04	0.07	0.08	0.19	0.31	0.36	0.41	0.42
3m	0.52	0.42	0.29	0.26	0.12	0.15	0.13	0.17	0.24	0.31	0.33
4m	0.72	0.64	0.55	0.53	0.36	0.37	0.24	0.21	0.20	0.25	0.27
5m	0.88	0.81	0.75	0.74	0.61	0.61	0.47	0.43	0.34	0.41	0.41
6m	1.00	0.95	0.90	0.91	0.81	0.80	0.69	0.68	0.59	0.62	0.65
7m	1.12	1.07	1.03	1.03	0.95	0.94	0.87	0.86	0.79	0.80	0.82
8m	1.21	1.17	1.15	1.16	1.08	1.06	1.00	1.00	0.94	0.95	0.98
9m	1.29	1.25	1.22	1.22	1.17	1.15	1.10	1.12	1.07	1.09	1.11

Table 10: MMD value between the healthy state data of turbine T2.1 and the remaining turbines at Farm 2 under both healthy and scoured states

Scour Depth	Target Turbines										
	T 2.1	T 2.2	T 2.3	T 2.4	T 2.5	T 2.6	T 2.7	T 2.8	T 2.9	T 2.10	T 2.11
0m (Healthy)	0.00	0.04	0.03	0.12	0.21	0.38	0.45	0.47	0.57	0.61	0.62
1m	0.03	0.01	0.01	0.05	0.12	0.28	0.36	0.38	0.50	0.55	0.56

https://doi.org/10.5194/wes-2026-70
Preprint. Discussion started: 23 April 2026

eawe european academy of wind energy
Open Access WIND ENERGY SCIENCE DISCUSSIONS

2m	0.14	0.05	0.07	0.03	0.05	0.15	0.21	0.24	0.38	0.44	0.45
3m	0.32	0.19	0.21	0.13	0.08	0.07	0.10	0.13	0.24	0.30	0.33
4m	0.50	0.36	0.37	0.32	0.20	0.11	0.12	0.12	0.15	0.19	0.21
5m	0.64	0.52	0.53	0.51	0.36	0.26	0.27	0.27	0.17	0.19	0.20
6m	0.76	0.66	0.66	0.67	0.53	0.44	0.48	0.47	0.34	0.35	0.31
7m	0.85	0.78	0.78	0.79	0.67	0.59	0.64	0.64	0.52	0.54	0.48
8m	0.90	0.89	0.89	0.90	0.78	0.73	0.78	0.77	0.68	0.69	0.63
9m	0.90	1.00	1.01	1.01	0.90	0.84	0.89	0.88	0.80	0.81	0.77

Table 11: MMD value between the healthy state data of turbine T3.1 and the remaining turbines at Farm 3 under both healthy and scoured states

Scour Depth	Target Turbines										
	T 3.1	T 3.2	T 3.3	T 3.4	T 3.5	T 3.6	T 3.7	T 3.8	T 3.9	T 3.10	T 3.11
0m (Healthy)	0.00	0.04	0.05	0.11	0.23	0.38	0.42	0.47	0.55	0.64	0.67
1 m	0.02	0.01	0.01	0.05	0.16	0.29	0.33	0.40	0.48	0.58	0.62
2 m	0.11	0.02	0.02	0.02	0.07	0.17	0.21	0.29	0.37	0.48	0.53
3 m	0.26	0.11	0.13	0.08	0.04	0.07	0.10	0.17	0.24	0.35	0.42
4 m	0.39	0.26	0.29	0.23	0.11	0.07	0.09	0.11	0.14	0.22	0.29
5 m	0.53	0.41	0.42	0.37	0.25	0.19	0.19	0.12	0.13	0.16	0.20
6 m	0.65	0.55	0.57	0.52	0.40	0.32	0.31	0.21	0.21	0.20	0.19
7 m	0.77	0.68	0.70	0.66	0.55	0.46	0.46	0.34	0.34	0.30	0.25
8 m	0.86	0.79	0.79	0.78	0.69	0.61	0.62	0.49	0.50	0.46	0.39
9 m	0.93	0.87	0.89	0.86	0.79	0.74	0.75	0.63	0.65	0.61	0.55

Table 12 reports the MMD distance between turbine T3.1 and the remaining turbines across all three farms in the healthy state. The results indicate that the inter-farm shift is larger than the intra-farm shift, as in Farm 3, the intra-farm shift increases progressively from turbines T3.1 to T3.11 due to variation in water depth and localised soil changes. Beyond these intra-farm shifts, a clear inter-farm shift is observed even between turbines installed at comparable water depths (e.g., T3.1, T2.1, and T1.1), demonstrating that differences in soil characteristics strongly influence the discrepancy in data distributions. The combined effect of inter-farm shift and intra-farm shift highlights a significant challenge in developing a fully generalised scour detection model capable of handling variations across different environmental and structural conditions.

Table 12: MMD distance between turbine T3.1 and the remaining turbines across different farms in the healthy state (X is 1-3 for farms 1-3)

	TX.1	TX.2	TX.3	TX.4	TX.5	TX.6	TX.7	TX.8	TX.9	TX.10	TX.11
Farm 3	0.00	0.04	0.05	0.11	0.23	0.38	0.42	0.47	0.55	0.64	0.67
Farm 2	0.71	0.73	0.73	0.80	0.82	0.90	0.96	0.96	0.98	1.02	1.00
Farm 1	1.15	1.15	1.17	1.21	1.23	1.19	1.21	1.26	1.27	1.29	1.28

https://doi.org/10.5194/wes-2026-70
Preprint. Discussion started: 23 April 2026

eawe european academy of wind energy
Open Access WIND ENERGY SCIENCE DISCUSSIONS

4. Results and discussion

In this section, the methodology explained in Section 2 is implemented and validated using the datasets generated in Section 3. First, the proposed generalised scour detection framework is validated through different training and testing protocols. This is followed by a sensitivity analysis to investigate the impact of sensor location choice on the proposed method's performance. Additionally, the sensitivity of the proposed model to the number of source turbines and their location within the farm is assessed. Finally, the impact of the choice of the DG model on the results is studied.

4.1 Global scour detection across different farms

In this section, the combined source turbine data is passed to a data loader, where it is stored in batches of 720 samples to ensure that each batch receives a data mixture from all three source domains during the training phase. This further encourages the network to learn both task-specific features and domain-invariant representations. The training process is designed to jointly optimise both the classification performance and the model's capability to generalise across turbines. A gradually adjusted learning rate is applied to both the feature extractor and the domain discriminator to stabilise the training process. A learning rate of 0.00075 is used for the classifier, while a learning rate of 0.001 is used for the domain discriminator. In each iteration, a batch of source-domain data is loaded, latent features are extracted through the shared network, and two losses are computed: (1) a classification loss, and (2) a domain confusion loss. The total loss based on the difference between these terms is used to promote domain confusion, while optimisation is carried out separately for both the classifier and domain discriminator. Subsequently, the model is evaluated at each iteration on source data, with early stopping applied to prevent overfitting, as the training progress is terminated when a drop in accuracy greater than 3% is observed. Throughout the training phase, the model's performance is logged at regular intervals by evaluating its accuracy on the target-domain data.

During the evaluation phase, the unseen target dataset is normalised using the corresponding reference turbine at the same farm and used to assess model accuracy at the final iteration. The model's capability for detecting various scour levels at the remaining previously unseen target turbines across the given farms is thoroughly assessed. This study employs multiple training and evaluation protocols, as described in Section 2.3, to assess the performance of the proposed framework across various practical scenarios. Table 13 presents the training protocols/ tasks used for the model development. In Task 1, the model is trained on data from the reference turbine, located in the shallow water with the lowest soil density within each farm (T1.1, T2.1, and T3.1). Task 2 and Task 3 extend this by training the model on turbines located at intermediate-water depths with medium soil density (T1.6, T2.6, and T3.6) and at deep water with the highest soil density (T1.11, T2.11, and T3.11), respectively. Additionally, Task 4 simulates challenging scenarios with mixed-source turbines installed at varying water depths (T1.1, T2.11, and T3.6).

Table 13: Training task specifications used for the model development

Task	Source Turbine	Target Turbine
Task 1	{T1.1 , T2.1 , T3.1 }	
Task 2	{T1.6 , T2.6 , T3.6 }	Farm 1 {T1.1- T1.11}, Farm 2 {T2.1- T2.11}, and Farm 3 {T3.1- T3.11}
Task 3	{T1.11 , T2.11 , T3.11 }	
Task 4	{T1.1 , T2.11 , T3.6 }	

Figure 5a- 5c illustrate the performance of the proposed model in identifying the scour state at target turbines located in Farms 1, 2, and 3, respectively. The results indicate that in Task 1, the model effectively detects scour states with scour depths ($S > 3$ m) around monopile foundations in Farm 1 and Farm 2. Whereas, its performance is reduced at Farm 3, particularly for the

https://doi.org/10.5194/wes-2026-70
Preprint. Discussion started: 23 April 2026

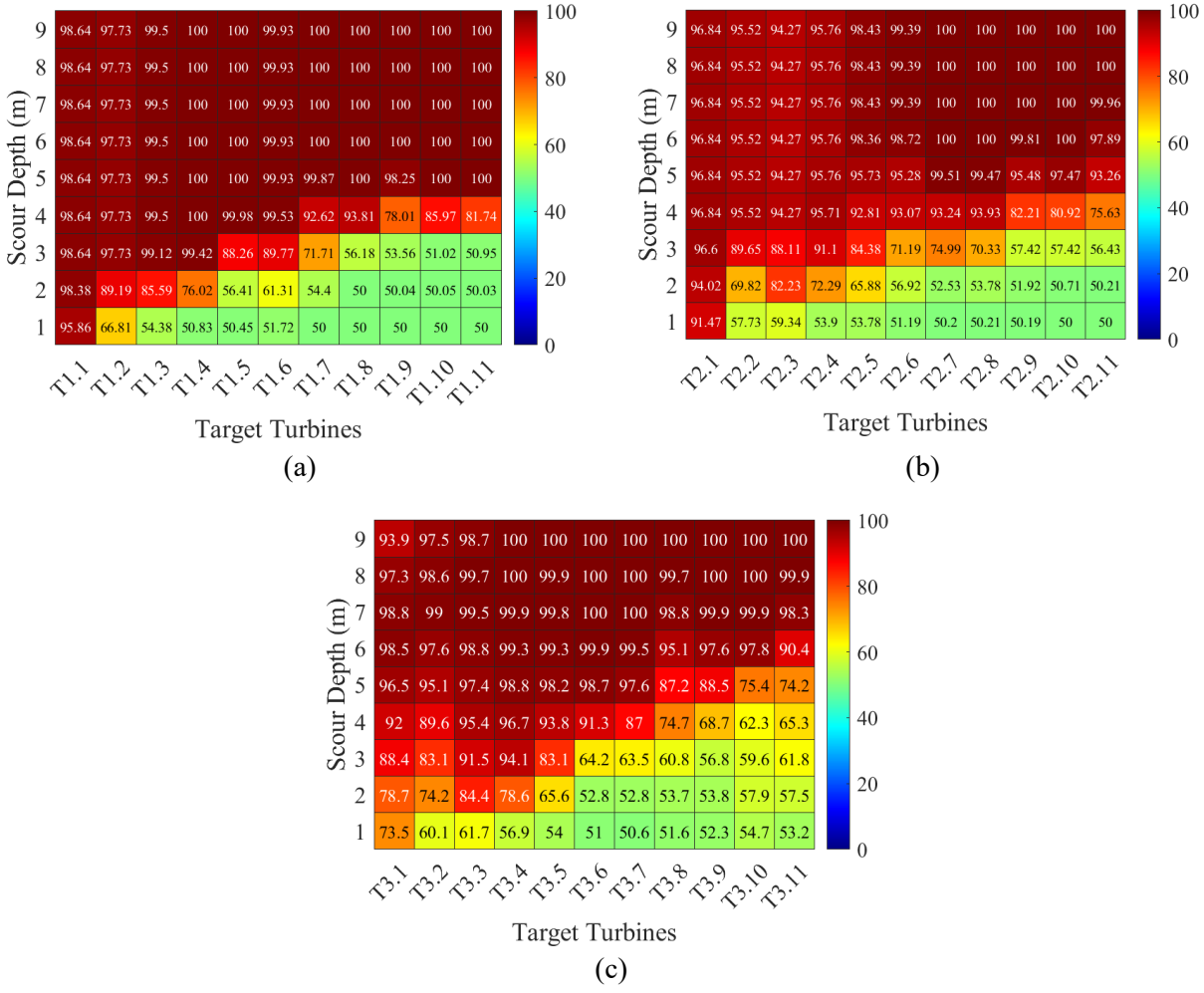

Figure 5: The proposed model performance when trained on Task 1 and evaluated on target OWTs located at a) Farm 1, b) Farm 2, and c) Farm 3.

Figures 6d- 6f illustrate the model's performance when trained on Task 2 and evaluated on the remaining target turbines across the given farms. In Task 2, the model exhibits low generalisation capability across wind farm units, with satisfactory accuracy limited to turbines closely matching the source conditions, particularly in terms of water depth and soil density. A similar trend is observed across all three wind farms, where turbines located at greater water depths than the source turbine are accurately identified. In contrast, the scour detection performance degrades for turbines in shallower water due to the distributional shift in data caused by differences in water depth and soil stiffness. These shifts lead to misclassification, with the model often incorrectly identifying a healthy state as scoured due to similarities between the source turbines' healthy state and the scoured state of the target turbines. Despite its limited performance for shallow water turbines (T1.1 – T1.5, T2.1 – T2.5, and T3.1 – T3.5), the model effectively detects scour in deep-water turbines, achieving accuracies above 90%.

https://doi.org/10.5194/wes-2026-70
Preprint. Discussion started: 23 April 2026

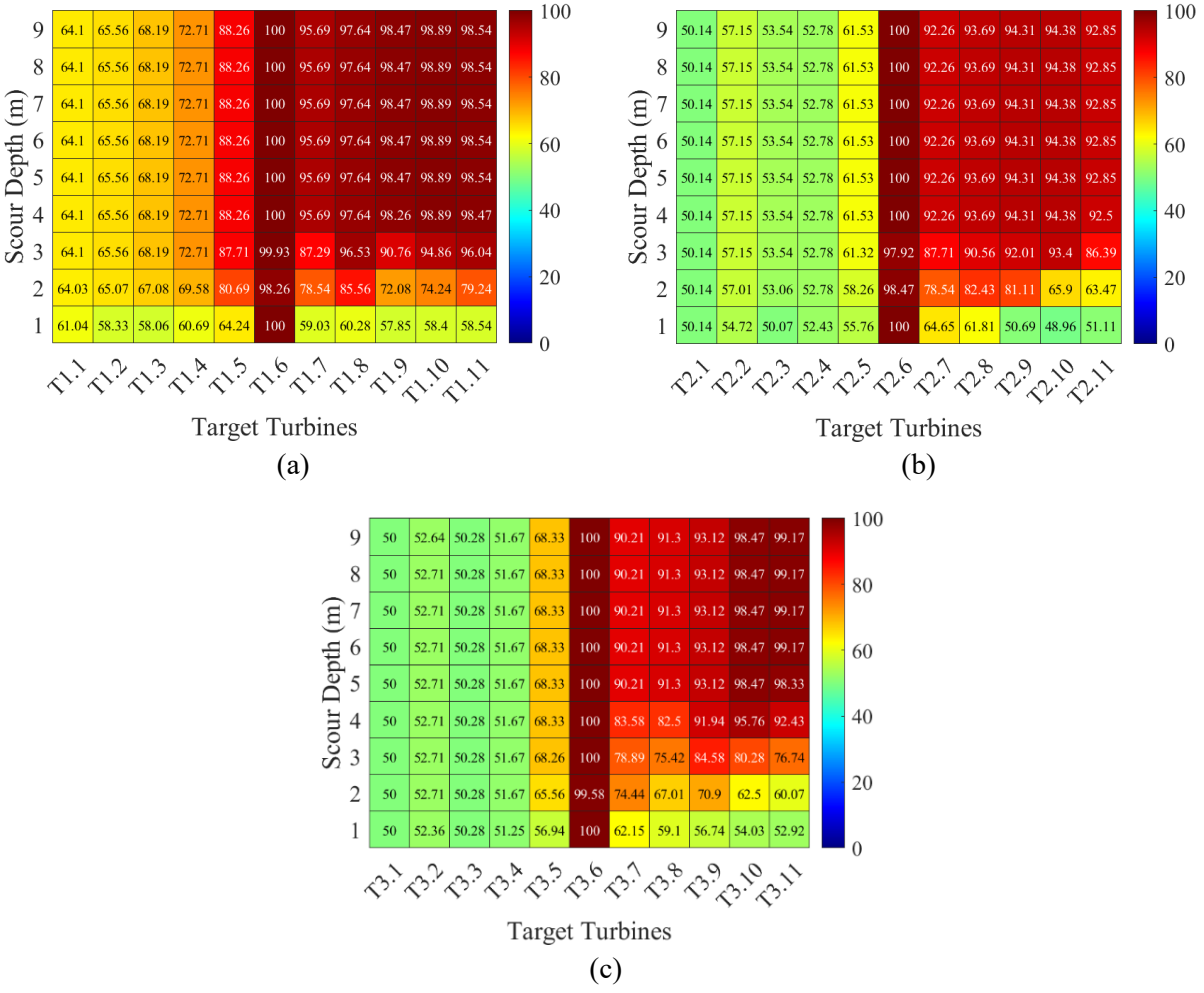

Figure 6: The proposed model performance when trained on Task 2 and evaluated on target OWTs located at a) Farm 1, b) Farm 2, and c) Farm 3

Figure 7g- 7i indicate the model accuracy when trained on Task 3 and evaluated on the remaining turbines across all three farms. The results show that model performance is strongly influenced by the source turbine location within each farm. Notably, scour detection at Farm 1 exhibits the most consistent results compared to Farm 2 and Farm 3. The model achieves acceptable accuracy for the four turbines closest to the source (T1.9 – T1.11); however, its accuracy drops sharply for turbines in shallower water, indicating limited generalisation across target turbines operating under different conditions. This reduction in accuracy can mainly be attributed to differences between the invariant features learned during training and those obtained during evaluation. A comparison across the different training tasks further reveals that using shallow-water turbines with lower soil stiffness as source domains consistently outperforms training on intermediate or deep-water turbines with higher soil stiffness, which indicates the importance of carefully selecting source turbines to maximise scour detection performance at wind farm scale.

https://doi.org/10.5194/wes-2026-70
Preprint. Discussion started: 23 April 2026

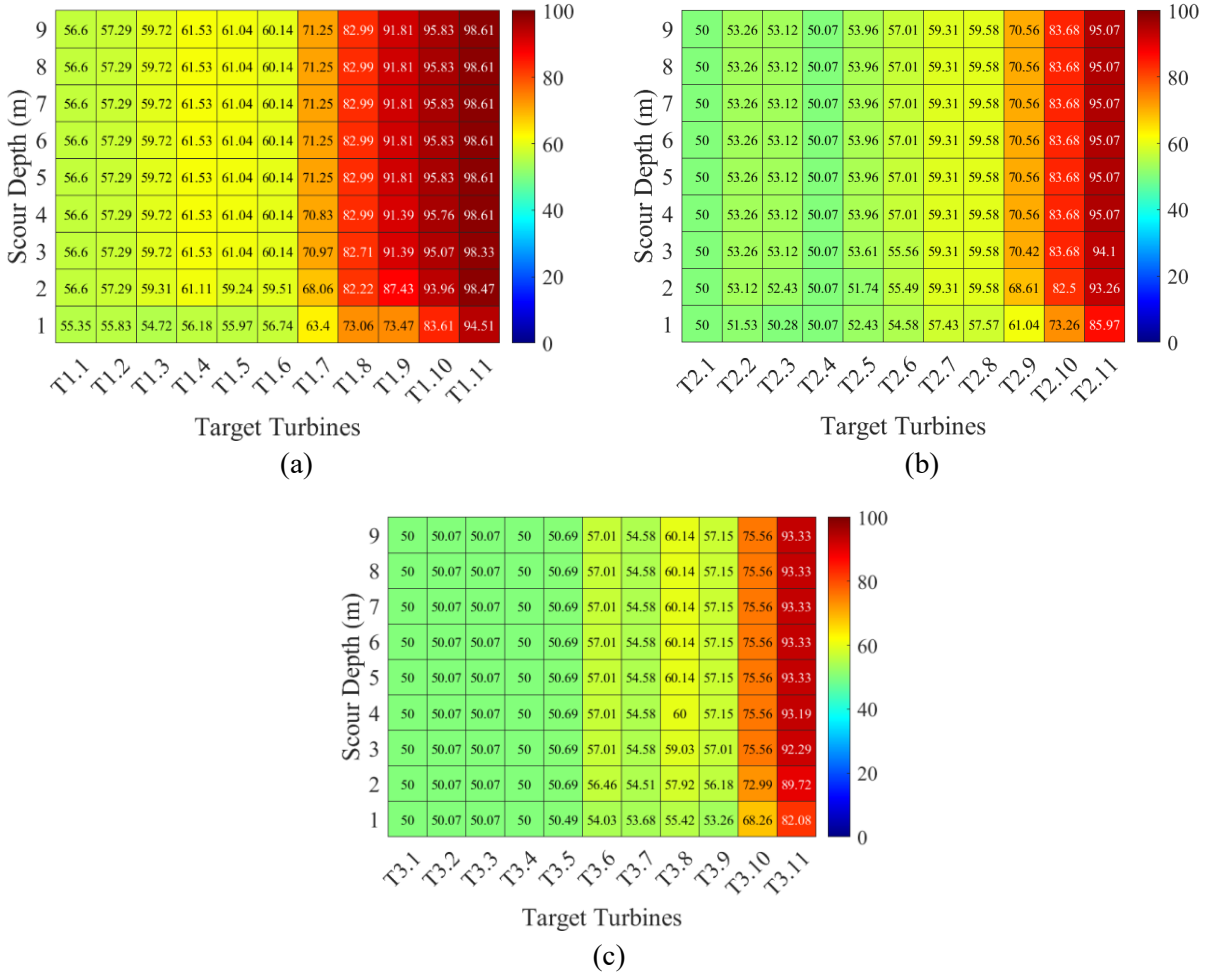

Figure 7: The proposed model performance when trained on Task 3 and evaluated on target OWTs located at a) Farm 1, b) Farm 2, and c) Farm 3

Figure 8j- 8l represent the results for the model's capacity trained on Task 4, and assessed across multiple target turbines. The results demonstrate that models trained on combined source data achieve higher scour detection accuracy when shallow water turbines with lower soil density are used as source domains. In contrast, performance decreases when intermediate or deep-water turbines with increased soil density are selected. This reduction in accuracy is primarily attributed to the model's limited capability to identify the healthy state, which is misclassified as scour due to distributional shifts. Overall, the model reliably detected scour for turbines installed at greater water depths, particularly those with higher soil stiffness than the training conditions.

https://doi.org/10.5194/wes-2026-70
Preprint. Discussion started: 23 April 2026

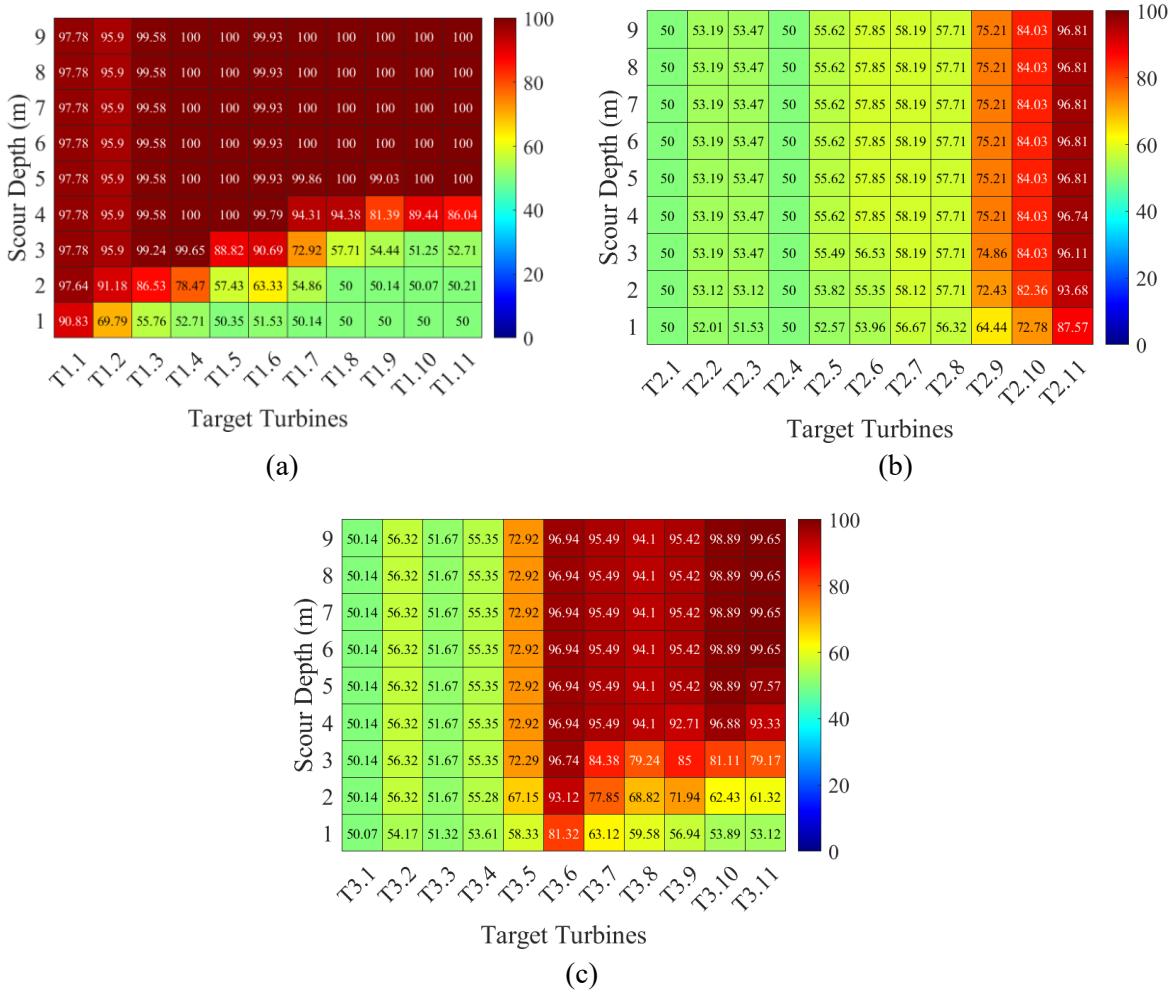

Figure 8: The proposed model performance when trained on Task 4 and evaluated on target OWTs located at a) Farm 1, b) Farm 2, and c) Farm 3

4.2 Model sensitivity to tower sensor positioning

To enhance the applicability of the proposed framework and evaluate the effectiveness of acceleration sensors at different locations, this section investigates the impact of sensor placement on model performance. Specifically, the model is re-evaluated using acceleration data collected at the tower top, instead of Sensor 1 located at the tower base. Consistent with earlier analyses, the model is trained on Task 1, with the architecture and hyperparameters kept constant. Table 14 represents the impact of sensor location on model performance, measured as the average scour detection accuracy across all target turbines in all given farms (T1.2 – T1.11, T2.1 – T2.11, and T3.1 – T3.11) over a range of scour depths. However, the performance may vary between individual OWTs; the average accuracy reflects the overall trend. The results show that, regardless of sensor location, the model performs well for larger scour depths ($S > 6$ m), demonstrating its strong potential for farm-level scour detection. However, the model trained using data collected at the tower base achieves higher accuracy for shallow and intermediate scour depths, particularly for in range $S = 3 - 6\,m$, highlighting that the tower base is a more effective sensor location. Primarily, the base-mounted sensor provides more stable performance across farms, with lower variability in

https://doi.org/10.5194/wes-2026-70
Preprint. Discussion started: 23 April 2026

eawe european academy of wind energy
Open Access WIND ENERGY SCIENCE DISCUSSIONS

detection accuracy compared to the tower-top sensor, particularly for turbines located further from the source conditions. Regardless of the sensor location, the model struggles to detect very shallow scour depths ($S = 1 - 2$ m), likely due to the minimal changes in acceleration response at early scour stages, which exhibits small scour depth compared to the pile length (L= 30m, 40m and 50 m for Farm 1, 2, and 3, respectively.

390 **Table 14: The impact of sensor location at the source turbines on the scour detection accuracy at the target turbines across the farms.**

Farm	Sensor Location		Average scour detection accuracy across the farm under different scour states (%)								
			1 m	2 m	3 m	4 m	5 m	6 m	7 m	8 m	9 m
Farm 1	Sensor 1	Avg.	56.4	65.6	77.9	93.4	99.5	99.6	99.6	99.6	99.6
		Std	14.0	18.3	21.3	8.00	0.80	0.80	0.80	0.80	0.80
	Sensor 2	Avg.	54.9	61.7	72.2	82.5	95.9	98.9	99.0	99.0	99.0
		Std	11.0	16.9	21.2	19.4	4.40	2.20	2.30	2.30	2.30
Farm 2	Sensor 1	Avg.	56.2	63.7	76.2	90.4	96.2	97.9	98.2	98.2	98.2
		Std	12.2	14.6	14.8	7.20	2.00	2.10	2.20	2.20	2.20
	Sensor 2	Avg.	54.2	60.9	68.2	76.9	88.4	96.3	98.0	98.3	98.3
		Std	7.90	14.9	19.6	18.7	13.1	3.70	2.80	2.80	2.80
Farm 3	Sensor 1	Avg.	56.3	64.6	73.4	83.4	91.6	97.6	99.5	99.6	99.1
		Std	6.80	12.2	14.5	13.0	9.20	2.70	0.60	0.90	1.90
	Sensor 2	Avg.	53.2	59.4	67.4	76.1	84.4	91.6	96.4	97.8	98.1
		Std	5.00	11.7	17.9	18.0	16.3	9.80	3.60	2.80	2.90

4.3 Sensitivity of model performance to the number of source turbines

This section examines the influence of source data volume and diversity on model accuracy and introduces an alternative
395 approach to improve the prediction performance for turbines located far from the source turbines. The effect of increasing the number of source turbines used for training the DG model is thoroughly investigated by expanding the source set from three to six turbines (T1.1, T1.6, T2.1, T2.6, T3.1, and T3.6). In this section, each target turbine is normalised with respect to its closest source turbine. Figure 9 presents the impact of the number of source turbines on model performance. The average accuracy across all turbines in the given wind farms is reported at different scour depths and compared with the results from
400 Section 4.2, where only three source turbines were employed. The results show that increasing the diversity of the source dataset significantly enhances model accuracy, particularly for shallow scour depths (S=2 m – 4 m), with a limited impact on deeper scour depths. These findings highlight the importance of source data volume and diversity, suggesting that increasing access to a wide set of source turbines enhances overall scour detection performance.

https://doi.org/10.5194/wes-2026-70
Preprint. Discussion started: 23 April 2026

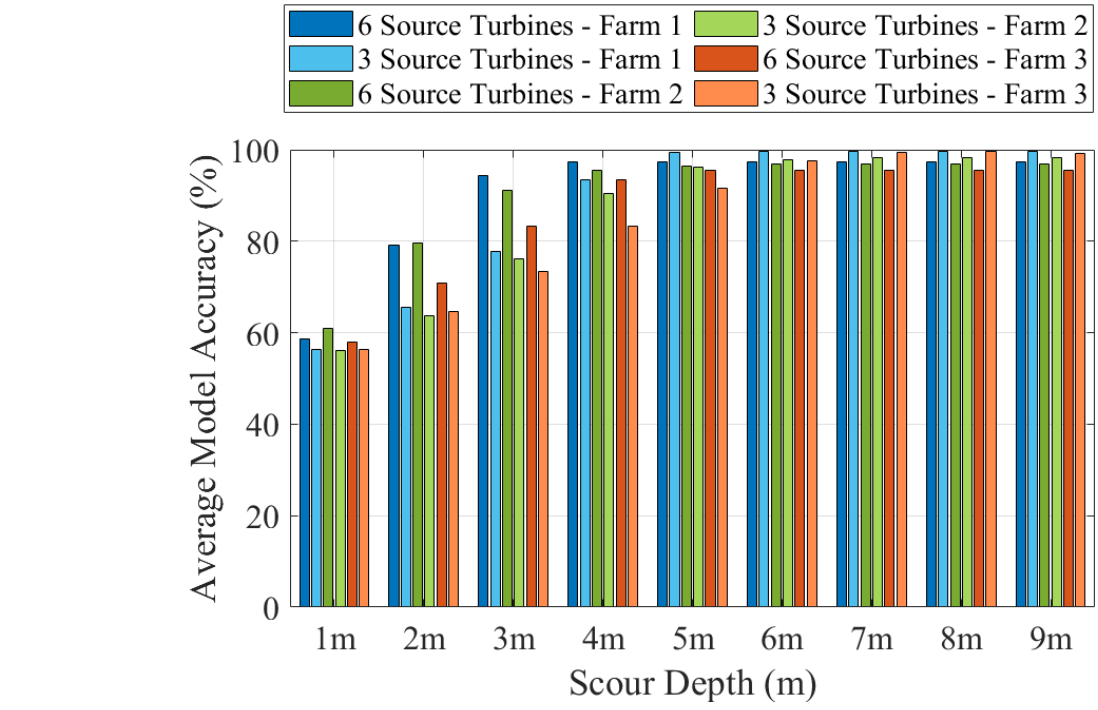

405 **Figure 9: The impact of the number of source turbines on the model performance**

4.4 Influence of the DG method on model behaviour

This section evaluates the impact of the chosen DG method on overall model performance by comparing the Causal Disentanglement Domain Generalisation (CDDG) approach (Ragab et al., 2022) with the DANN framework for scour
410 detection. The CDDG method is designed to learn domain-invariant features that generalise to previously unseen target domains by combining classification loss with conditional contrastive loss. This formulation encourages the similarity between features of the same class at different domains, while minimising the similarity between different classes. For the feature extractor, a 1D CNN is employed, with an architecture consistent with that used in the DANN model. To ensure a fair comparison, the source turbines, network architecture, and hyperparameters are kept identical for both methods, with the
415 average performance of CCDG vs. DANN method for scour detection at Farms 1, 2, and 3 is compared as shown in Figure 10. The results reveal that both DG models achieve high detection accuracy, with only minor differences in performance. At Farm 1, both models exhibit comparable results; however, CCDG has better accuracy in detecting shallow scour depths at Farms 2 and 3, whereas DANN performs better in detecting larger scour depths.

https://doi.org/10.5194/wes-2026-70
Preprint. Discussion started: 23 April 2026

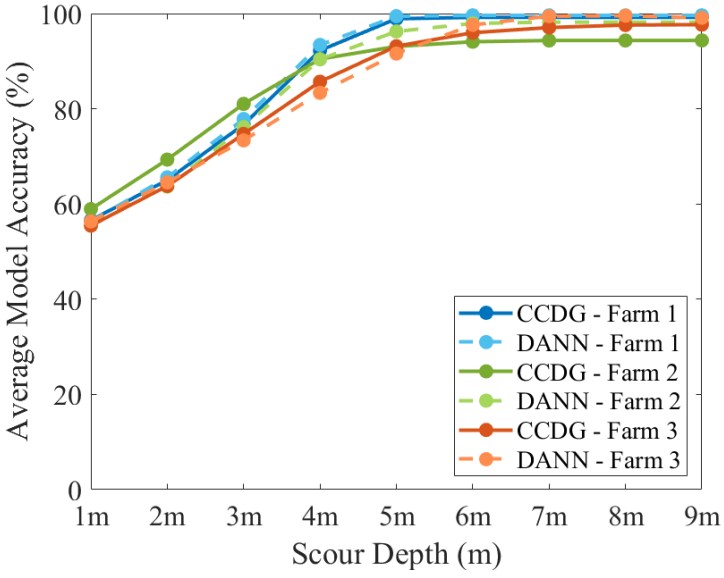

Figure 10: The impact of the selected DG method on the model performance

The present study is limited to a hypothetical wind farms, where the site conditions are assumed to vary uniformly across turbines with a specified range of scour depths. It is further assumed that the soil density changes with water depth, which is restricted to a range of 20-25m for the considered wind farms. Due to the restriction on data availability, the validation of the proposed framework is based on numerically generated datasets obtained using a coupled OpenFAST and SSI model; therefore, variations in model performance may occur when the proposed approach is applied to real-world measurements. Additionally, the analysis is limited to the predefined operational and environmental conditions using an NREL 5MW turbine model. These conditions replicate the typical normal operational conditions, with sea currents modelled theoretically rather than actual measurements. Therefore, further changes in model performance may be anticipated when applied to field data.

5. Conclusion

This study proposes a general framework for scour detection at the inter-offshore wind farm level. The framework primarily relies on the domain generalisation model, developed using early installation data obtained from a single sensor at an individual reference turbine per farm. Training on the combined source dataset, obtained from three farms, evaluates the model's capacity for scour detection at the remaining previously unseen target turbines, with the following results obtained.

- The model trained on source turbines located in shallow water with lower soil densities demonstrates strong potential for generalised scour detection at different target turbines with higher soil properties across the three farms. However, models trained on intermediate or deep-water turbines with higher soil densities show reduced generalisation capability.

https://doi.org/10.5194/wes-2026-70
Preprint. Discussion started: 23 April 2026

- The model excels for scour detection across farms when developed on datasets obtained from the shallowest and lowest stiffness foundations. However, training the model on scenarios with increased water depth and higher stiffness foundations resulted in reduced performance.
- Models developed using tower base sensor data outperform those based on tower top sensors, highlighting that the tower bottom is the optimal sensor placement for effective scour detection.
- Increasing the number of source turbines has a notable impact on enhancing the model performance, specifically at shallow scour depths.
- Both DANN and CCDG domain generalisation methods maintain high performance for generalised scour detection, successfully detecting intermediate and deep scour depths but failing to detect shallow scour depths of 1 m.

This study is limited to three hypothetical wind farms, each comprising 11 OWT units. The effect of increasing the number of farms and unit locations on the model performance necessitates further investigation. Additionally, the impact of incorporating alternative feature types on model performance requires further assessment. Future work should also explore the use of other domain generalisation methods to mitigate data shifts, as well as the potential of training and testing across different farms to evaluate the model's generalisation capacity better.

Author contributions

Mahmoud Abdelhak: Writing – original draft, Visualization, Validation, Software, Methodology, Formal analysis, Data curation, Conceptualization. **Luke J. Prendergast**: Writing – review & editing, Project administration, Methodology, Funding acquisition, Conceptualization. **Jacques Tott-Buswell**: Software, Methodology, Data curation. **Ramin Ghiasi**: Writing – review & editing, Validation, Supervision, Methodology**. Abdollah Malekjafarian**: Writing – review & editing, Visualization, Supervision, Project administration, Methodology, Funding acquisition, Conceptualization.

Declaration of competing interest

The authors declare that they have no known competing financial interests or personal relationships that could have appeared to influence the work reported in this paper.

Acknowledgements

The authors from the University of Nottingham are grateful for the financial support provided by UKRI through Innovate UK and the KTP initiative.

Data availability

Data will be made available on request.

https://doi.org/10.5194/wes-2026-70
Preprint. Discussion started: 23 April 2026

eawe european academy of wind energy
Open Access WIND ENERGY SCIENCE DISCUSSIONS

References

Abdelhak, M., Prendergast, L. J., Tott-Buswell, J., Ghiasi, R., & Malekjafarian, A. (2026). Wind farm-level scour detection around offshore monopile foundations using unsupervised domain adaptation. Mechanical Systems and Signal Processing, 251, 114186. https://doi.org/10.1016/j.ymssp.2026.114186

Abdelhak, M., Tott-Buswell, J., Prendergast, L. J., Ghiasi, R., & Malekjafarian, A. (2025). Scour identification around offshore wind turbine monopile foundations using an unsupervised anomaly detection approach. Ocean Engineering, 340, 122365. https://doi.org/10.1016/j.oceaneng.2025.122365

Arany, L. S., Bhattacharya, S., Macdonald, J. H. G., & Hogan, S. J. (2017). Design of monopiles for offshore wind turbines in 10 steps. Soil Dynamics and Earthquake Engineering, 92, 126–152.

Cao, W., et al. (2025). A bearing fault diagnosis method for unknown operating conditions based on differentiated feature extraction. ISA Transactions, 156, 468–478. https://doi.org/10.1016/j.isatra.2024

Cieslak, M. C., Castelfranco, A. M., Roncalli, V., Lenz, P. H., & Hartline, D. K. (2020). t-distributed stochastic neighbor embedding (t-SNE): A tool for eco-physiological transcriptomic analysis. Marine Genomics, 51, 100723. https://doi.org/10.1016/j.margen.2019.100723

Dai, S., Han, B., Wang, B., Luo, J., & He, B. (2021). Influence of soil scour on lateral behavior of large-diameter offshore wind-turbine monopile and corresponding scour monitoring method. Ocean Engineering, 239, 109809. https://doi.org/10.1016/j.oceaneng.2021.109809

Dayal, A., KB, V., Cenkeramaddi, L. R., Mohan, C., Kumar, A., & Balasubramanian, V. N. (2023). MADG: Margin-based adversarial learning for domain generalization. Advances in Neural Information Processing Systems, 36, 58938–58952.

DNV GL. (2016). Loads and site conditions for wind turbines (DNVGL-ST-0437). http://www.dnvgl.com

Duan, B., Wang, D., Qin, C., & Duan, L. (2025). Local scour around marine structures: A comprehensive review of influencing factors, prediction methods, and future directions. Buildings, 15(12), 2125. https://doi.org/10.3390/buildings15122125

Ganin, Y., & Lempitsky, V. S. (2014). Unsupervised domain adaptation by backpropagation. In International Conference on Machine Learning.

Ghojogh, B., & Ghodsi, A. (2024). Maximum mean discrepancy and generative moment matching networks: Tutorial and survey. Retrieved from https://hal.science/hal-04723220

Ghojogh, B., Ghodsi, A., Karray, F., & Crowley, M. (2021). Reproducing kernel Hilbert space, Mercer's theorem, eigenfunctions, Nyström method, and use of kernels in machine learning: Tutorial and survey. arXiv preprint arXiv:2106.08443.

Huang, W. H., & Yang, R. Y. (2021). Water depth variation influence on the mooring line design for FOWT within shallow water region. Journal of Marine Science and Engineering, 9(4). https://doi.org/10.3390/jmse9040409

Jatoliya, A., Bhattacharya, D., Manna, B., Bento, A. M., & Fazeres-Ferradosa, T. (2024). Physics-based and machine-learning models for accurate scour depth prediction. Philosophical Transactions of the Royal Society A, 382(2264), 20220403. https://doi.org/10.1098/rsta.2022.0403

Jawalageri, S., Ghiasi, R., Jalilvand, S., Prendergast, L. J., & Malekjafarian, A. (2024). A data-driven approach for scour detection around monopile-supported offshore wind turbines using Naive Bayes classification. Marine Structures, 95, 103565. https://doi.org/10.1016/j.marstruc.2023.103565

Jeong, S., Kim, E. J., Shin, D. H., Park, J. W., & Sim, S. H. (2020). Data fusion-based damage identification for a monopile offshore wind turbine structure using wireless smart sensors. Ocean Engineering, 195, 106728. https://doi.org/10.1016/j.oceaneng.2019.106728

Jonkman, J., Butterfield, S., Musial, W., & Scott, G. (2009). Definition of a 5-MW reference wind turbine for offshore system development. National Renewable Energy Laboratory. http://www.osti.gov/bridge

Juo, D.-J., Chang, W.-Y., & Wu, I. H. (2021). Windowing techniques, the Welch method for improvement of power spectrum estimation. Computers, Materials & Continua, 67, 3983–4003. https://doi.org/10.32604/cmc.2021.014752

Ju, X., Wu, X., Dai, S., Li, M., & Hu, D. (2025). Domain adversarial learning with multiple adversarial tasks for EEG emotion recognition. Expert Systems with Applications, 266, 126028. https://doi.org/10.1016/j.eswa.2024.126028

https://doi.org/10.5194/wes-2026-70
Preprint. Discussion started: 23 April 2026

Li, X., Zhang, W., Ma, H., Luo, Z., & Li, X. (2020). Domain generalization in rotating machinery fault diagnostics using deep neural networks. Neurocomputing, 403, 409–420. https://doi.org/10.1016/j.neucom.2020.05.014

Lin, C., Han, J., Bennett, C., & Parsons, R. L. (2016). Analysis of laterally loaded piles in soft clay considering scour-hole dimensions. Ocean Engineering, 111, 461–470. https://doi.org/10.1016/j.oceaneng.2015.11.029

Lu, B., et al. (2024). Visual deep learning with physics constraints for local scour evolution prediction at monopiles. Journal of Ocean Engineering and Science. https://doi.org/10.1016/j.joes.2024.04.001

Mostafa, Y. E. (2012). Effect of local and global scour on lateral response of single piles in different soil conditions. Engineering, 4(6), 297–306. https://doi.org/10.4236/eng.2012.46039

Najafzadeh, M., Bento, A. M., Basirian, S., & Fazeres-Ferradosa, T. (2025). Dynamic damage functions for scour protection at monopile foundations: Application of ensemble machine learning models. Ocean Engineering, 323, 120590. https://doi.org/10.1016/j.oceaneng.2025.120590

Niu, X., Chen, X., Du, W., Xie, A., & Wang, H. (2023). Method for monitoring scour depth of monopile under different relative densities of soil. Ships and Offshore Structures, 18(10), 1438–1447. https://doi.org/10.1080/17445302.2022.2120298

Prendergast, L. J., Gavin, K., & Doherty, P. (2015). An investigation into the effect of scour on the natural frequency of an offshore wind turbine. Ocean Engineering, 101, 1–11. https://doi.org/10.1016/j.oceaneng.2015.04.017

Prendergast, L. J., Reale, C., & Gavin, K. (2018). Probabilistic examination of the change in eigenfrequencies of an offshore wind turbine under progressive scour incorporating soil spatial variability. Marine Structures, 57, 87–104. https://doi.org/10.1016/j.marstruc.2017.09.009

Ragab, M., et al. (2022). Conditional contrastive domain generalization for fault diagnosis. IEEE Transactions on Instrumentation and Measurement, 71, 1–12. https://doi.org/10.1109/TIM.2022.3154000

Teng, S., Chen, G., Yan, Z., Cheng, L., & Bassir, D. (2023). Vibration-based structural damage detection using 1-D convolutional neural network and transfer learning. Structural Health Monitoring, 22, 2888–2909. https://doi.org/10.1177/14759217221137931

Wang, X., Zeng, X., Li, J., Yang, X., & Wang, H. (2018). A review on recent advancements of substructures for offshore wind turbines. Energy Conversion and Management, 158, 103–119. https://doi.org/10.1016/j.enconman.2017.12.061

Weijtjens, W., Verbelen, T., Capello, E., & Devriendt, C. (2017). Vibration-based structural health monitoring of the substructures of five offshore wind turbines. Procedia Engineering, 199, 2294–2299. https://doi.org/10.1016/j.proeng.2017.09.187